

photoelectron data offers definite advantages.

**Acknowledgment.** The samples used in this study have been kindly supplied by Professor R. H. Martin (Université Libre de Bruxelles). It is a pleasure to thank him and Professor E. Heilbronner (Universität Basel) for valuable discussions and for reading the manuscript and Professor H. Nöth (Universität München) for the permission to use his photoelectron spectrometer.

**Supplementary Material Available.** Spectra for benzene, naphthalene, phenanthrene, 3,4-benzophenanthrene, and the higher homologs will appear following these pages in the microfilm edition of this volume of the journal. Photocopies of the supplementary material from this paper only or microfiche (105 × 148 mm, 24X reduction, negatives) containing all of the supplementary material for the papers in this issue may be obtained from the Business Office, Books and Journals Division, American Chemical Society, 1155 16th St., N.W., Washington, D.C. 20036. Remit check or money order for \$4.00 for photocopy or \$2.50 for microfiche, referring to code number JACS-75-6633.

## References and Notes

- (1) For reviews see: (a) R. H. Martin, *Angew. Chem., Int. Ed. Engl.*, **13**, 649 (1974); (b) R. H. Martin, "Aromaticity, Pseudo-Aromaticity and Antiaromaticity", E. D. Bergmann and B. Pullman, Ed., *The Israel Academy of Sciences and Humanities*, 1971, p 115.
- (2) (a) R. H. Martin, M. Flammang-Barbieux, J. P. Cosyn, and M. Gelbcke, *Tetrahedron Lett.*, 3507 (1968); (b) R. H. Martin, G. Morren, and J. J. Schurter, *ibid.*, 3683 (1969); (c) R. H. Martin et al., unpublished.
- (3) G. W. Frank, D. T. Hefelfinger, and D. A. Lightner, *Acta Crystallogr., Sect. B*, **29**, 223 (1973).
- (4) C. de Rango, G. Tsoucaris, J. P. Declercq, G. Germain, and J. P. Putzeys, *Cryst. Struct. Commun.*, **2**, 189 (1973).
- (5) I. R. MacKay, J. M. Robertson, and J. G. Sime, *Chem. Commun.*, 1470 (1969).
- (6) W. Rhodes and M. F. A. El-Sayed, *J. Mol. Spectrosc.*, **9**, 42 (1962).
- (7) (a) O. E. Weigang, J. A. Turner, and P. A. Trouard, *J. Chem. Phys.*, **45**, 1126 (1966); (b) O. E. Weigang and P. A. Trouard, *ibid.*, **49**, 4248 (1968).
- (8) (a) A. Brown, C. M. Kemp, and S. F. Mason, *J. Chem. Soc. A*, 751 (1971); (b) W. S. Brickell, A. Brown, C. M. Kemp, and S. F. Mason, *ibid.*, 756 (1971).
- (9) M. S. Newman, R. S. Darlak, and L. Tsai, *J. Am. Chem. Soc.*, **89**, 6191 (1967).
- (10) V. Boekelheide and W. Schmidt, *Chem. Phys. Lett.*, **17**, 410 (1972).
- (11) E. Heilbronner and J. P. Maier, *Helv. Chim. Acta*, **57**, 151 (1974).
- (12) E. Vander Donckt, J. Nasielski, J. R. Greenleaf, and J. B. Birks, *Chem. Phys. Lett.*, **2**, 409 (1968).

- (13) (a) M. B. Robin, "Higher Excited States of Polyatomic Molecules", Academic Press, New York, N.Y., 1974; (b) W. Schmidt, submitted for publication.
- (14) R. Boschi, E. Clar, and W. Schmidt, *J. Chem. Phys.*, **60**, 4406 (1974).
- (15) D. W. Turner, "Molecular Photoelectron Spectroscopy", Wiley, London, 1970, p 271.
- (16) P. A. Clark, F. Brogli, and E. Heilbronner, *Helv. Chim. Acta*, **55**, 1415 (1972).
- (17) J. H. D. Eiland, *Int. J. Mass Spectrom. Ion Phys.*, **9**, 214 (1972).
- (18) R. Boschi, J. N. Murrell, and W. Schmidt, *Discuss. Faraday Soc.*, **54**, 116 (1972).
- (19) F. Brogli and E. Heilbronner, *Angew. Chem., Int. Ed. Engl.*, **11**, 538 (1972).
- (20) R. E. Christoffersen, unpublished results.
- (21) K. Seki, H. Inokuchi, and Y. Harada, *Chem. Phys. Lett.*, **20**, 197 (1973), and earlier papers quoted therein.
- (22) A. J. Moscovitz, Ph.D. Thesis, Harvard University, 1957.
- (23) G. Wagnière, ref 1b, pp 127 and 138.
- (24) E. Heilbronner, *Tetrahedron Lett.*, 1923 (1964).
- (25) H. Hope, J. Bernstein, and K. N. Trueblood, *Acta Crystallogr., Sect. B*, **28**, 1733 (1972).
- (26) A. W. Hanson, *Acta Crystallogr., Sect. B*, **28**, 2287 (1972).
- (27) D. J. Cram and J. M. Cram, *Acc. Chem. Res.*, **4**, 204 (1971).
- (28) R. H. Martin and M. J. Marchant, *Tetrahedron*, **30**, 347 (1974); for the racemization of [5]helicene see C. Goedicke and H. Stegemeyer, *Tetrahedron Lett.*, 937 (1970).
- (29) H. Wynberg, W. C. Nieuwpoort, and H. T. Jonkman, *Tetrahedron Lett.*, 4623 (1973).
- (30) E. Clar, "Polycyclic Aromatic Hydrocarbons", Vol. I, Academic Press, New York, N.Y., 1964.
- (31) M. Flammang-Barbieux, J. Nasielski, and R. H. Martin, *Tetrahedron Lett.*, 743 (1967).
- (32) R. H. Martin and M. J. Marchant, *Tetrahedron*, **30**, 343 (1974).
- (33) NOTE ADDED IN PROOF. The optical spectra of [10]- to [14]helicene are at present under investigation in the laboratories of J. B. Birks (The University, Manchester) and E. VanDer Donckt (Université Libre de Bruxelles). The energies of the p bands (from the absorption spectra) and  $\alpha$  bands (measured on the fluorescence spectra and increased by 0.12 eV in order to compensate for the Stokes shift between the absorption and emission spectra) are, after correcting for the gas phase:

	$E_{\alpha}$	$E_p$
[10] Helicene	2.73	3.26 ± 0.06
[11] Helicene	2.67	3.16 ± 0.06
[12] Helicene	2.61	3.07 ± 0.06
[13] Helicene	2.57	3.03 ± 0.06
[14] Helicene	2.57	3.03 ± 0.06

Thus, the  $\alpha$  band is the first transition in the optical spectra. Comparison with the calculated transition energies in Table III shows good agreement for the  $\alpha$  bands; the experimental  $E_p$  values quoted above are again too high by one or two quanta in the CC stretching mode. We thank Professors Birks and VanDer Donckt for communicating their data to us in advance of publication.

## Microwave Spectrum, Molecular Structure, and Dipole Moment of Oxaspiro[2.2]pentane

Warren D. Slafer,<sup>1a</sup> Alan D. English,<sup>1a</sup> David O. Harris,<sup>\*1a</sup> Dale F. Shellhamer,<sup>1b</sup> Michael J. Meshishnek,<sup>1b</sup> and Donald H. Aue<sup>1b</sup>

Contribution from the Quantum Institute and the Department of Chemistry, University of California, Santa Barbara, California 93106. Received April 4, 1975

**Abstract:** The assignment of microwave spectrum of oxaspiro[2.2]pentane, **1**, and its <sup>13</sup>C and monodeuterio isotopically substituted derivatives is reported. These data are sufficient to permit the determination of the complete molecular structure. Measurement of a large number of microwave transitions allowed the quartic centrifugal distortion parameters to be calculated for the parent and each of the isotopic species. The Stark effect was used to obtain the two components of the electric dipole moment, giving  $\mu_a = 0.840 \pm 0.012$  D,  $\mu_c = 1.721 \pm 0.004$  D, and  $\mu_{total} = 1.915 \pm 0.009$  D.

Oxaspiro[2.2]pentane, **1**, and its derivatives have only recently been prepared; their chemistry has received increasing attention in recent years<sup>2</sup> because of interest in the unusually strained bonding, hybridization, and reactivity of

this ring system and because of their potential as synthetic intermediates.<sup>2a,c</sup>

The structure and dipole moment of oxaspiro[2.2]pentane is of interest in relation to the related oxirane,<sup>3</sup> cyclo-

propane,<sup>4</sup> and spiro[2.2]pentane<sup>5</sup> structures in the literature. The microwave bond angles and NMR <sup>13</sup>C-<sup>13</sup>C and <sup>13</sup>C-H coupling constants in these systems provide complementary information about the hybridization in these strained rings.<sup>6</sup>

## Experimental Section

The microwave spectra were taken on a Hewlett-Packard 8460A microwave spectrometer equipped with P and K bands (12.3 to 26.5 GHz). Although oxaspiropentane is very stable in methylene chloride solution, it decomposes in the pure state at room temperature. Consequently most spectra were taken with the Stark cell cooled to Dry Ice temperature. Final purification was by vapor phase chromatography, after which the sample was stored in a base-washed vacuum bulb in liquid nitrogen. Under these conditions, the useful lifetime of a sample was several weeks. Experiments could be carried out for several hours in the cold cell before appreciable degradation of the sample occurred; however, at room temperature the useful lifetime was less than 30 min. The degree of decomposition was monitored by observing the relative intensity of a cyclobutanone<sup>7</sup> line which is one of the decomposition products.

Stark cell pressures ranged from 1 to 60 mTorr, with the higher pressures being used for initial assignment of the weaker isotopic species.

Nuclear magnetic resonance spectra were obtained on a Varian T-60 spectrometer; infrared spectra were obtained on a Perkin-Elmer 337 spectrophotometer. Gas chromatography was performed on a Varian Aerograph Model A-700 or Model 920 gas chromatograph equipped with a thermal conductivity detector. Mass spectra were recorded on a Finnigan 1015 quadrupole mass spectrometer.

**Oxaspiro[2.2]pentane (1).** To a 250-ml flask was added 50 ml of dichloromethane, 15 g of commercial *m*-chloroperbenzoic acid (85%), and 30 g of anhydrous sodium bicarbonate. The mixture was cooled to 0° under nitrogen and 3.3 g of methylenecyclopropane (**2a**) in 25 ml of dichloromethane was added at once. The flask was stoppered tightly and stirred at 15° for 3 hr. The flask was cooled to 0° and the contents bulb-to-bulb distilled into a Dry Ice trap. The dichloromethane solution of the epoxide was dried over sodium sulfate and stored at -10°. The epoxide was purified by preparative VPC on a 6 ft × 0.25 in. column of 15% SE-30 on 60-80 Chromosorb W,  $T_R^{25^\circ} = 18$  min. The yield of **1** was 53% plus 4% recovered olefin by VPC analysis.

**2,2,3,3-Polydeuteriomethylenecyclopropanes (2b).** Into a 200 ml flask fitted with a Teflon stopcock, 1.5 g of methylenecyclopropane was vacuum transferred from sodium hydride. To a 100-ml flask was added, under nitrogen, 350 mg of sodium hydride (55% dispersion in mineral oil). The hydride was washed with petroleum ether and 12 g of dimethyl sulfoxide-*d*<sub>6</sub> added under nitrogen. This mixture was stirred at 75° for 1 hr under nitrogen and the resulting solution freeze degassed. The methylenecyclopropane was vacuum transferred into the reaction flask and the flask was sealed with a threaded Teflon stopcock. The mixture was stirred at 25° for 36 hr. Vacuum transfer of the volatile products gave 1.3 g (82%) of the deuteriomethylenecyclopropanes, **2b**, containing 76% deuterium by NMR analysis. Analysis by mass spectrometry indicated 77% deuterium (4% *d*<sub>1</sub>, 19% *d*<sub>2</sub>, 41.5% *d*<sub>3</sub>, 35.5% *d*<sub>4</sub>).

The deuteriomethylenecyclopropanes were oxidized in a manner similar to that for methylenecyclopropane and stored as solutions in dichloromethane. The oxaspiro[2.2]pentanes were purified by preparative VPC as needed.

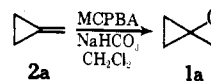
Oxaspiro[2.2]pentanes used in the microwave studies were prepared from batches of methylenecyclopropanes, **2b**, containing 20% deuterium (44% *d*<sub>0</sub>, 36% *d*<sub>1</sub>, 16% *d*<sub>2</sub>, 4% *d*<sub>3</sub>, 0% *d*<sub>4</sub>), and methylenecyclopropanes, **2c**, containing 12% *d* (62.5% *d*<sub>0</sub>, 28.5% *d*<sub>1</sub>, 8.5% *d*<sub>2</sub>, 0.5% *d*<sub>3</sub>, 0% *d*<sub>4</sub>).

**Thermolysis of 2,2,3,3-Polydeuteriomethylenecyclopropanes (2b).** To a 2-l. pyrolysis bulb was vacuum transferred 5.5 g of deuteriomethylenecyclopropane, **2b**, containing 12% deuterium. The bulb was sealed and placed in an oven at 235° for 13 hr. The cooled bulb was opened under nitrogen flow and the methylenecyclopropane was vacuum transferred to a storage flask: NMR (CCl<sub>4</sub>) δ 1.03 (s, 4 H, CH<sub>2</sub>-CH<sub>2</sub>), 5.38 (s, 2 H, =CH<sub>2</sub>). Analysis of the product by NMR showed complete scrambling of deuterium

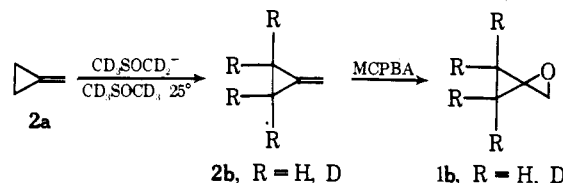
with peaks at δ 1.03 and 5.38 integrating 93:46. No other volatile products or polymer was observed in these reactions.

## Preparation of Oxaspiro[2.2]pentanes

Oxaspiropentane, **1a**, was prepared by oxidation of methylenecyclopropane, **2a**, with *m*-chloroperbenzoic acid (MCPBA) at 15° in methylene chloride solvent in 53% yield.<sup>2a,b</sup> A substitution microwave structure of **1a** required the preparation of species **1b** and **1c** with deuterium substituents in the 2, 3, and 4 positions.

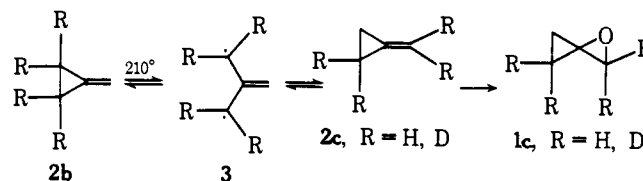


Deuterium substitution in the 3,4 positions of oxaspiro[2.2]pentane was accomplished by exchange of the allylic hydrogens in the 2,3 positions of methylenecyclopropane to give **2b**. The deuterium exchange occurs readily at 25° with



the sodium salt of dimethyl sulfoxide-*d*<sub>6</sub> generated from the reaction of sodium hydride with dimethyl sulfoxide-*d*<sub>6</sub> as solvent.

Thermal isomerization of the deuteriomethylenecyclopropanes **2b** via the interesting trimethylenemethane diradical **3**<sup>8</sup> provides a pathway to the scrambled species **2c** required for preparation of the 2,3-polydeuteriooxaspiro[2.2]pentanes, **1c**. Such an isomerization was readily accomplished at 235° in the gas phase. The rate of this isomerization of **2b** to **2c** was found to be  $2.6 \times 10^{-5} \text{ sec}^{-1}$  at 209.5°.<sup>9</sup>



Polydeuteriooxaspiropentanes **1b** and **1c** were readily prepared by these methods. Mixtures with a high percentage of *d*<sub>1</sub> species were used for the microwave studies.

## Microwave Spectral Assignment

Structural calculations based on assumed parameters for oxaspiropentane were carried out to determine an initial set of rotational constants and predict the microwave spectrum. These calculations indicated the molecule to be an accidental near prolate top with a  $\kappa$  value of about -0.95 and having both *a*- and *c*-type transitions. In addition to the usual <sup>a</sup>*R*<sub>01</sub> series, a large number of *c*-type transitions were predicted to fall within the accessible spectral region.

The observed spectrum was found to be quite dense and due almost entirely to the stronger perpendicular *c*-dipole component. The *c*-dipole 0<sub>0,0</sub> → 1<sub>1,0</sub> transition was observed within several hundred megahertz of the predicted frequency and confirmed by its characteristic Stark effect. The *a*-dipole 2 → 3 transitions were then identified and the assignment partially completed.

A number of extremely intense, regularly spaced lines initially remained unexplained. With the aid of a centrifugal distortion analysis, these were subsequently identified as members of high *J* <sup>c</sup>*Q* branch series. The complete set of measured transitions used to determine the final rotational parameters for the <sup>12</sup>C species is given in Table I.

Table I. Rotational Transition Frequencies and Centrifugal Distortion Corrections in  $^{12}\text{C}$ -Oxaspiro[2.2]pentane

Transition	Calcd freq <sup>a</sup>	Centrifugal distortion <sup>b</sup>	Obsd freq	Obsd - calcd	Transition	Calcd freq <sup>a</sup>	Centrifugal distortion <sup>b</sup>	Obsd freq	Obsd - calcd
$0_{0,0} \rightarrow 1_{1,0}$	16011.67	-0.02	16011.69	0.02	$17_{1,16} \rightarrow 17_{2,16}$	16383.75	-3.51	16383.77	0.02
$1_{0,1} \rightarrow 2_{1,1}$	24801.18	-0.06	24801.18	-0.00	$18_{1,17} \rightarrow 18_{2,17}$	15788.36	-4.02	15788.38	0.02
$1_{0,1} \rightarrow 2_{0,2}$	17431.28	-0.03	17431.29	0.01	$23_{1,22} \rightarrow 23_{2,22}$	12533.29	-6.77	12533.26	-0.03
$1_{1,0} \rightarrow 2_{1,1}$	17505.44	-0.05	17505.47	0.03	$31_{18,13} \rightarrow 32_{17,15}$	24899.54	28.02	24899.57	0.03
$1_{1,1} \rightarrow 2_{1,2}$	17358.22	-0.03	17358.22	0.00	$31_{18,14} \rightarrow 32_{17,16}$	24899.54	28.02	24899.57	0.03
$2_{1,1} \rightarrow 2_{2,1}$	21666.30	-0.10	21666.28	-0.02	$34_{2,32} \rightarrow 34_{3,32}$	22949.07	-44.28	22949.04	-0.03
$2_{1,1} \rightarrow 3_{1,2}$	26257.76	-0.12	26257.76	0.00	$38_{25,13} \rightarrow 39_{24,15}$	15616.32	-126.84	15616.33	0.01
$2_{1,2} \rightarrow 2_{2,0}$	21887.70	-0.12	21887.73	0.03	$38_{25,14} \rightarrow 39_{24,16}$	15616.32	-126.84	15616.33	0.01
$2_{1,2} \rightarrow 3_{1,3}$	26036.93	-0.09	26036.92	-0.01	$40_{26,14} \rightarrow 41_{25,16}$	12687.75	-139.82	12687.76	0.00
$2_{2,0} \rightarrow 3_{2,1}$	26149.89	-0.15	26149.88	-0.01	$40_{26,15} \rightarrow 41_{25,17}$	12687.75	-139.82	12687.76	0.00
$2_{2,1} \rightarrow 3_{2,2}$	26147.64	-0.16	26147.68	0.04	$43_{28,15} \rightarrow 44_{27,17}$	15536.57	-177.35	15536.58	0.01
$3_{1,2} \rightarrow 3_{2,2}$	21556.18	-0.14	21556.18	-0.01	$43_{28,16} \rightarrow 44_{27,18}$	15536.57	-177.35	15536.58	0.01
$3_{1,3} \rightarrow 3_{2,1}$	22000.65	-0.19	22000.64	-0.01	$44_{26,18} \rightarrow 45_{25,20}$	22147.23	103.90	22147.23	0.00
$3_{2,2} \rightarrow 4_{1,4}$	12717.33	-0.01	12717.36	0.03	$44_{26,19} \rightarrow 45_{25,21}$	22147.23	103.90	22147.23	0.00
$4_{1,4} \rightarrow 4_{2,2}$	22154.08	-0.27	22154.08	0.00	$44_{29,15} \rightarrow 45_{28,17}$	21312.66	-203.18	21312.67	0.01
$5_{1,5} \rightarrow 5_{2,3}$	22350.40	-0.38	22350.38	-0.02	$44_{29,16} \rightarrow 45_{28,18}$	21312.66	-203.18	21312.67	0.01
$5_{3,2} \rightarrow 6_{2,4}$	16032.31	-0.09	16032.30	-0.01	$48_{29,19} \rightarrow 49_{28,21}$	13515.52	160.82	13515.49	-0.02
$5_{3,3} \rightarrow 6_{2,5}$	15993.12	-0.21	15993.12	0.00	$48_{29,20} \rightarrow 49_{28,22}$	13515.52	160.82	13515.49	-0.02
$5_{5,1} \rightarrow 6_{4,3}$	13030.82	-1.01	13030.80	-0.02	$48_{31,17} \rightarrow 49_{30,19}$	15444.98	-239.70	15444.99	0.01
$6_{3,4} \rightarrow 7_{2,6}$	24701.38	-0.51	24701.40	0.02	$48_{31,18} \rightarrow 49_{30,20}$	15444.98	-239.70	15444.99	0.01
$6_{6,0} \rightarrow 7_{5,3}$	18831.63	-1.92	18831.61	-0.03	$50_{30,20} \rightarrow 51_{29,22}$	16445.17	174.78	16445.14	-0.03
$6_{6,1} \rightarrow 7_{5,3}$	18831.63	-1.92	18831.61	-0.03	$50_{30,21} \rightarrow 51_{29,23}$	16445.17	174.78	16445.14	-0.03
$8_{1,7} \rightarrow 8_{2,7}$	20463.20	-0.63	20463.21	0.01	$50_{32,18} \rightarrow 51_{31,20}$	12509.82	-259.26	12509.86	0.04
$8_{5,3} \rightarrow 9_{4,5}$	13122.11	0.17	13122.13	0.02	$50_{32,19} \rightarrow 51_{31,21}$	12509.82	-259.26	12509.86	0.04
$10_{6,4} \rightarrow 11_{5,6}$	16037.87	0.32	16037.88	0.01	$51_{30,21} \rightarrow 52_{29,23}$	25149.92	161.66	25149.91	-0.01
$10_{6,5} \rightarrow 11_{5,7}$	16037.87	0.32	16037.88	0.01	$51_{30,22} \rightarrow 52_{29,24}$	25149.92	161.66	25149.91	-0.01
$10_{8,2} \rightarrow 11_{7,4}$	12998.62	-4.21	12998.58	-0.04	$51_{33,18} \rightarrow 52_{32,20}$	18278.28	-292.74	18278.27	-0.01
$10_{8,3} \rightarrow 11_{7,5}$	12998.62	-4.21	12998.58	-0.04	$51_{33,19} \rightarrow 52_{32,21}$	18278.28	-292.74	18278.27	-0.01
$12_{10,2} \rightarrow 13_{9,4}$	24597.04	-9.29	24597.02	-0.02	$52_{34,18} \rightarrow 53_{33,20}$	24044.34	-328.59	24044.31	-0.03
$12_{10,3} \rightarrow 13_{9,5}$	24597.04	-9.29	24597.02	-0.02	$52_{34,19} \rightarrow 53_{33,21}$	24044.34	-328.59	24044.31	-0.03
$13_{2,11} \rightarrow 13_{1,13}$	25929.90	-1.92	25929.89	-0.01	$53_{33,50} \rightarrow 53_{4,50}$	25187.51	-207.24	25187.53	0.02
$13_{8,5} \rightarrow 14_{7,7}$	13152.35	1.92	13152.39	0.04	$53_{32,21} \rightarrow 54_{31,23}$	13603.35	219.40	13603.33	-0.02
$13_{8,6} \rightarrow 14_{7,8}$	13152.35	1.92	13152.39	0.04	$53_{32,22} \rightarrow 54_{31,24}$	13603.35	219.40	13603.33	-0.02
$13_{10,3} \rightarrow 14_{9,5}$	15880.69	-8.49	15880.67	-0.02	$55_{33,22} \rightarrow 56_{32,24}$	16536.23	236.60	16536.20	-0.03
$13_{10,4} \rightarrow 14_{9,6}$	15880.69	-8.49	15880.67	-0.02	$55_{33,23} \rightarrow 56_{32,25}$	16536.23	236.60	16536.20	-0.03
$14_{8,6} \rightarrow 15_{7,8}$	21869.77	0.82	21869.79	0.02	$57_{35,54} \rightarrow 57_{4,54}$	19869.77	-226.68	19869.75	-0.02
$14_{8,7} \rightarrow 15_{7,9}$	21869.77	0.82	21869.79	0.02	$57_{34,23} \rightarrow 58_{33,25}$	19469.88	254.56	19469.86	-0.02
$14_{11,4} \rightarrow 15_{10,6}$	21679.00	-11.95	21678.97	-0.03	$57_{34,24} \rightarrow 58_{33,26}$	19469.88	254.56	19469.87	-0.02
$14_{11,3} \rightarrow 15_{10,5}$	21679.00	-11.95	21678.97	-0.03	$61_{35,58} \rightarrow 61_{4,58}$	14929.85	-228.00	14929.85	-0.00
$15_{1,14} \rightarrow 15_{2,14}$	17499.94	-2.60	17499.87	0.03	$63_{3,60} \rightarrow 63_{4,60}$	12697.76	-220.77	12697.77	0.01
$15_{9,6} \rightarrow 16_{8,8}$	16068.79	2.62	16068.82	0.03	$65_{39,26} \rightarrow 66_{38,28}$	16758.72	400.59	16758.75	0.03
$15_{9,7} \rightarrow 16_{8,9}$	16068.79	2.62	16068.82	0.03	$65_{39,27} \rightarrow 66_{38,29}$	16758.72	400.59	16758.75	0.03
$15_{11,4} \rightarrow 16_{10,6}$	12962.82	-10.87	12962.80	-0.02	$72_{43,29} \rightarrow 73_{42,31}$	19838.22	535.15	19838.25	0.03
$15_{11,5} \rightarrow 16_{10,7}$	12962.82	-10.87	12962.80	-0.02	$72_{43,30} \rightarrow 73_{42,32}$	19838.22	535.15	19838.25	0.03
$16_{1,15} \rightarrow 16_{2,15}$	16954.89	-3.04	16954.91	0.02					

<sup>a</sup>Frequency calculated using Hamiltonian correct to first order in centrifugal distortion. See text. <sup>b</sup>Centrifugal distortion term is added to rigid rotor frequency to give calculated frequency.

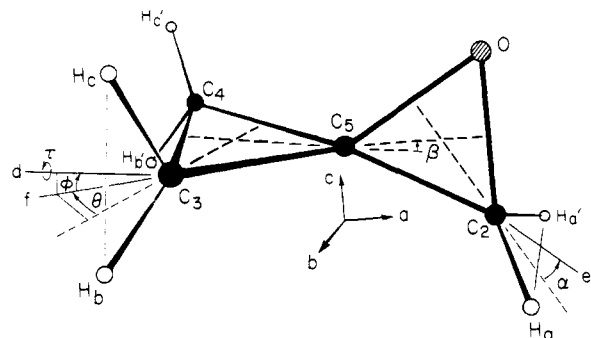


Figure 1. Oxaspiro[2.2]pentane, showing internal parameters. The heavy dashed lines represent angle bisectors and the lighter dashed lines the bisector extensions. Lines "d" and "e" are the bisectors of the  $\text{H C}_3\text{H}$  and  $\text{H C}_2\text{H}$  methylene groups, respectively. Line "f" is the projection of line "d" onto the  $\text{C}_3\text{C}_4\text{C}_5$  plane. The angles  $\theta$ ,  $\phi$ ,  $\tau$ , and  $\alpha$  describe the orientations of the methylene groups, and angle  $\beta$  is the relative tilt of one ring with respect to the other, as described in Table V. The relative orientation of the principal axes is also shown.

Because of its near symmetric nature, the energy level pattern of oxaspiropentane is characterized by numerous near degeneracies which were very useful in assigning the

weaker naturally occurring  $^{13}\text{C}$  isotopic species. Many of the transitions involving these levels were modulated at Stark fields small enough ( $\sim 10$  V/cm) to prevent modulation of the second-order Stark transitions. Under these conditions the spectrum was cleared of many strong lines that would otherwise have interfered with the observation and measurement of the weak  $^{13}\text{C}$  lines, while leaving only those involving the near degeneracies.

Initial predictions of the spectra of the three  $^{13}\text{C}$  species from substitution at  $\text{C}_2$ ,  $\text{C}_3$ , and  $\text{C}_5$  (Figure 1) were based on diagnostic least-squares<sup>10</sup> calculations. This technique allows the determination of a best guess set of parameters when insufficient experimental data are available to permit a conventional least-squares analysis. These calculations indicated that for the  $^{13}\text{C}_3$  (or  $^{13}\text{C}_4$ ) and  $^{13}\text{C}_2$  isotopes (2.2 and 1.1% natural abundances, respectively), the low  $J^c\text{Q}_{1,0}$  and  $^c\text{Q}_{1,2}$  series would provide the best opportunity for initial assignments. These lines were predicted to be relatively strong and to exhibit varying first-order Stark effects. The ensuing search was hampered by the large number of  $^{12}\text{C}$  lines that also occurred in this region. It was noted, however, that the distinctive shape of the partially modulated Stark envelope at low voltages was nearly identical for par-

Table II. Parameters<sup>a</sup> for the Isotopic Species of Oxaspiro[2.2]pentane

	Parent	<sup>13</sup> C <sub>2</sub>	<sup>13</sup> C <sub>5</sub>
<i>A</i>	11616.911 ± 0.002	11497.045 ± 0.005	11614.440 ± 0.004
<i>B</i>	4394.777 ± 0.001	4314.287 ± 0.002	4394.981 ± 0.001
<i>C</i>	4321.157 ± 0.001	4259.635 ± 0.002	4321.662 ± 0.001
<i>I<sub>a</sub></i>	43.503475	43.95703	43.51273
<i>I<sub>b</sub></i>	114.99469	117.14009	114.98934
<i>I<sub>c</sub></i>	116.95387	118.64301	116.94019
<i>κ</i>	-0.97982	-0.98490	-0.97989
<i>τ<sub>aaaa</sub></i> <sup>b</sup>	-0.03104 ± 0.00008	-0.03066 ± 0.00011	-0.03094 ± 0.00009
<i>τ<sub>bbbb</sub></i>	-0.00305 ± 0.00001	-0.00288 ± 0.00001	-0.00305 ± 0.00001
<i>τ<sub>cccc</sub></i>	-0.00278 ± 0.00001	-0.00269 ± 0.00001	-0.00280 ± 0.00001
<i>τ<sub>aabb</sub></i>	-0.01799 ± 0.00001	-0.01717 ± 0.00010	-0.01800 ± 0.00009
<i>τ<sub>bbcc</sub></i>	-0.00426 ± 0.00001	-0.00404 ± 0.00001	-0.00423 ± 0.00001
<i>σ</i> <sup>c</sup>	0.024	0.025	0.017
Lines <sup>d</sup>	89	42	43

	<sup>13</sup> C <sub>3,4</sub>	<sup>2</sup> H <sub>a</sub>	<sup>2</sup> H <sub>b</sub>	<sup>2</sup> H <sub>c</sub>
<i>A</i>	11464.034 ± 0.005	11124.967 ± 0.002	11015.749 ± 0.002	11030.490 ± 0.003
<i>B</i>	4334.695 ± 0.002	4258.849 ± 0.001	4280.715 ± 0.001	4293.265 ± 0.001
<i>C</i>	4242.230 ± 0.002	4169.958 ± 0.001	4155.955 ± 0.001	4170.073 ± 0.001
<i>I<sub>a</sub></i>	44.08361	45.42719	45.87759	45.81628
<i>I<sub>b</sub></i>	116.58856	118.66493	118.05879	117.71367
<i>I<sub>c</sub></i>	119.12979	121.19451	121.60287	121.19116
<i>κ</i>	-0.97439	-0.97444	-0.96363	-0.96409
<i>τ<sub>aaaa</sub></i>	-0.02978 ± 0.00016	-0.02851 ± 0.00008	-0.02754 ± 0.00011	-0.02665 ± 0.00023
<i>τ<sub>bbbb</sub></i>	-0.00292 ± 0.00002	-0.00324 ± 0.00001	-0.00313 ± 0.00001	-0.00320 ± 0.00003
<i>τ<sub>cccc</sub></i>	-0.00260 ± 0.00002	-0.00283 ± 0.00001	-0.00268 ± 0.00002	-0.00274 ± 0.00004
<i>τ<sub>aabb</sub></i>	-0.01696 ± 0.00016	-0.01547 ± 0.00007	-0.01561 ± 0.00011	-0.01616 ± 0.00023
<i>τ<sub>bbcc</sub></i>	-0.00410 ± 0.00001	-0.00282 ± 0.00001	-0.00335 ± 0.00001	-0.00343 ± 0.00001
<i>σ</i>	0.023	-0.016	0.014	0.023
Lines	43	70	59	53

<sup>a</sup> Rotational constants and centrifugal distortion constants have units of MHz. Moments of inertia are in amu Å<sup>2</sup>. Conversion factor used is 505376 amu Å<sup>2</sup> MHz. <sup>b</sup> *τ<sub>aacc</sub>* set equal to 0.0. <sup>c</sup> Standard deviation of least-squares fit. <sup>d</sup> Number of transitions used in fit.

ent and isotope, and their comparison ultimately led to the proper assignment of the Q-branch lines.

The R-branch lines were much weaker than those of the Q-branch for all of the isotopes and were initially difficult to locate. The R-branch assignment was aided by noting that for oxaspiropentane the  $\pm K$  doublet splittings become resolvable at *J* values of about 7 or greater, with the magnitude of the splittings being relatively insensitive to small variations in the rotational constants. Very careful scanning revealed the weak doublets and permitted the completion of the <sup>13</sup>C<sub>3,4</sub> and <sup>13</sup>C<sub>2</sub> assignments.

The <sup>13</sup>C<sub>5</sub> (1.1%) isotope offered additional complications arising from the fact that the C<sub>5</sub> atom lies very close to the molecule's center of mass. Due to the resulting similarity in rotational constants between parent and isotope (Table II), most of the isotopic low *J* transitions were unresolvable from those of the parent. The Q-branch fit was initially made on high *J* lines which were sufficiently shifted to be resolved. The R-branch lines for the <sup>13</sup>C<sub>5</sub> isotope were located by taking advantage of the fact that the C<sub>5</sub> atom lies in a plane formed by two principal axes. As described below, the information obtained from the Q branch could then be used to calculate a set of rotational constants *without* R-branch assignment. Spectra generated from these rotational constants greatly facilitated subsequent observation of the desired R-branch transitions.

The general procedure followed in locating isotopic lines consisted of including the parameters from each newly assigned species in the diagnostic least-squares calculation and predicting refined spectra for the remaining ones. This technique proved very useful in the assignment of the deuterated species.

The three monodeuterio oxaspiropentanes were present in a 28% d<sub>1</sub> sample of **1c** containing 9% each of species substituted at H<sub>a</sub>, H<sub>b</sub>, and H<sub>c</sub> (see Figure 1). The spectrum of the mixture of parent and deuterated species was directly compared to that of the parent under the same experimen-

tal conditions, allowing immediate identification of the transitions associated with the deuterated molecules.

A careful search for <sup>18</sup>O transitions with natural abundance 0.2% was carried out in order to complete the structural investigation. Calculated line strengths indicated that several of the strongest Q-branch series should be observable. Because the oxygen atom is also located in a principal axis plane, it was hoped that a Q-branch assignment alone could be used to estimate the three rotational constants, as was done with the <sup>13</sup>C<sub>5</sub> species. Although several lines were identified, the very low intensity combined with the severe problem of numerous overlapping intense transitions prevented measurement of a sufficiently large set of lines to confirm an assignment.

Isotopic assignments were completed without observation of distinct Stark components. The spectral features primarily relied upon in identifying a particular transition were the intensity and shape of the unresolved Stark envelope. Varying the zero-based Stark voltage at values well below that required for complete modulation produced distinctive line shapes which were nearly identical for isotope and parent, allowing elimination of incorrect isotopic transitions from consideration. While the intensities, Stark pattern, and quality of the fit are sufficient to confirm the isotopic assignments, additional tests were conducted to eliminate any possible ambiguities.

The possible erroneous assignment of a vibrational satellite as one of the weak <sup>13</sup>C species was ruled out by making intensity measurements at -78°C and at room temperature. For a vibrational state at -78°C having a population of 1% of the ground state, a Boltzmann calculation showed that the population would increase by a factor of about 5 upon warming to room temperature. Isotope/parent intensity ratios were measured at both temperatures and found to be nearly constant for all isotopes, thus eliminating the possible misassignment of vibrational satellites as isotopic species.

Symmetry considerations were also used to verify certain isotopic assignments. For substitution of an atom in a plane formed by two principal axes, the following relation holds:<sup>11</sup>

$$\Delta I_\alpha + \Delta I_\beta - \Delta I_\gamma = 0 \quad (1)$$

where  $\Delta I_\alpha$  is the difference in moments of inertia of the parent and isotope for the  $\alpha$  principal axis, and  $\gamma$  is the principal axis perpendicular to the plane. As this expression is valid only for rigid molecules, vibrational effects can cause the left side of the equation to differ from zero. Nevertheless, for the  $^{13}\text{C}_2$  and  $^{13}\text{C}_5$  isotopes, the experimental values of  $\Delta I_a + \Delta I_c - \Delta I_b$  are 0.0027 and  $-0.0009$ , respectively, and are sufficiently small to confirm their location in the symmetry plane.

In these instances, the inertial defect can also be used to obtain rotational constants when only a Q-branch assignment is available. Since the Q branch determines two linear combinations of the three rotational constants,<sup>12</sup> eq 1 supplies a third relationship and allows the complete determination of the three rotational constants. These rotational constants will differ from those determined by complete assignment of both Q and R branches by an amount which depends upon the size of the vibrational effect in eq 1. Comparison of the rotational constants and coordinates as calculated from this method and from the complete assignment is presented in Table III. A complete list of assigned transitions for the six isotopic species is given in the microfilm edition as Tables IA through VIA.

**Centrifugal Distortion.** The large number of high  $J$  lines assigned in the spectrum of oxaspiropentane made it feasible to obtain quartic centrifugal distortion parameters for the parent as well as for the isotopic species. The effects of the systematic errors introduced into the structure by centrifugal distortion are also minimized by using rotational constants that have been at least partially corrected for this effect.

The analysis is based on the first-order perturbation treatment of Kivelson and Wilson,<sup>13</sup> where the Hamiltonian is given as

$$\begin{aligned} H &= H_R + H_D \\ H_R &= AP_a^2 + BP_b^2 + CP_c^2 \\ H_D &= \frac{\hbar^2}{4} \sum_{\alpha, \beta, \gamma, \delta} \tau_{\alpha\beta\gamma\delta} P_\alpha P_\beta P_\gamma P_\delta \end{aligned} \quad (2)$$

where  $A = \hbar^2/2I_a$ , etc., and  $\alpha, \beta, \gamma, \delta = a, b, \text{ or } c$ . The experimentally observed rotational parameters are related to the parameters in the above Hamiltonian as follows:<sup>14</sup>

$$\begin{aligned} A' &= A - \frac{\hbar^4}{4} (2\tau_{abab} + 2\tau_{caca} - 3\tau_{bcbc}) \\ B' &= B - \frac{\hbar^4}{4} (2\tau_{bcbc} + 2\tau_{abab} - 3\tau_{caca}) \\ C' &= C - \frac{\hbar^4}{4} (2\tau_{bcbc} + 2\tau_{caca} - 3\tau_{abab}) \\ \tau'_{\alpha\alpha\beta\beta} &= \hbar^4 (\tau_{\alpha\alpha\beta\beta} + 2\tau_{\alpha\beta\alpha\beta}); \alpha \neq \beta \\ \tau'_{\alpha\alpha\alpha\alpha} &= \hbar^4 \tau_{\alpha\alpha\alpha\alpha} \end{aligned} \quad (3)$$

In order to obtain the  $\tau$  free (unprimed) rotational constants, the  $\tau_{\alpha\beta\alpha\beta}$ 's are needed; however, only linear combinations of the  $\tau_{\alpha\alpha\beta\beta}$ 's and  $\tau_{\alpha\beta\alpha\beta}$ 's are determined experimentally. Hirose<sup>3</sup> has pointed out that the  $\tau_{\alpha\beta\alpha\beta}$  terms are usually small and that their differences for various isotopes of the same molecule would be even smaller. Because Kraitchman's equations<sup>11</sup> use differences in moments of inertia, the error introduced into the structure by neglect of the  $\tau$  correction is expected to be minimal. Structural calculations similar to those discussed in the following section

were carried out using rotational constants obtained from a rigid rotor fit of the low  $J$  transitions for each isotope. The resulting structural parameters were compared with those obtained from similar calculations using rotational constants obtained from the centrifugal distortion fit of the data, and the differences were found to be quite small and well within the stated error limits for the structural parameters.

In order for the distortion constants to be well determined, lines from as many different Q- and R-branch families as possible were measured. For the parent species,  $a$ - and  $c$ -type lines from 11 R-branch and 5 Q-branch series (89 transitions total) were included in the final fit. Although some extremely weak high  $J$   $^a$ Q-branch transitions were predicted, none could be found. For the 1 and 2%  $^{13}\text{C}$  isotopes, observations were limited to transitions with maximum  $J$  values in the 30's and 40's, as the intensity decrease above these values prevented further measurements. Examination of the statistics generated by the fitting procedure indicated that the least-squares matrix was well determined by the data, as were all 8 of the experimental parameters.

The first-order theory appears to be adequate to describe the centrifugal distortion effects, with the overall standard deviation of the fit being comparable to the experimental measurement error.<sup>14</sup> Several lines with abnormally large deviations were reexamined and found to have been either part of an unresolved multiplet or misassigned. As oxaspiropentane is a fairly rigid molecule, the centrifugal distortion effects were expected to be relatively small. For the highest transition measured ( $72_{43,30} \rightarrow 73_{42,32}$ ) the distortion was found to be just over 500 MHz.

### Structure Calculations

The assignment of the parent and six singly substituted isotopic species permitted a complete determination of the structure. From these data, the coordinates of each of the substituted atoms in the principal axis system of the parent isotope can be calculated by use of Kraitchman's equations.<sup>11</sup> Because complete isotopic substitution was not possible, the moment equations were needed.

In addition to two nonzero oxygen coordinates, two other coordinates could not be determined using Kraitchman's equations. The  $\text{C}_5$  atom is close to the center of mass and gave an imaginary  $a$  coordinate. The  $\text{C}_{3,4}$  atom also yielded an imaginary  $c$  coordinate due to its proximity to the  $a$ - $b$  plane.

Of the nine moment equations available for a general asymmetric top, due to symmetry only five give nontrivial solutions for oxaspiropentane. Solution of the five equations yielded the four coordinates undetermined by Kraitchman's equations. The final set of coordinates is given in Table IV. The stated errors are strictly experimental, propagated from the errors in the measured rotational constants. However, in the case of the four coordinates derived from the moment equations, the errors were determined from the deviations of the least-squares fit.

Because the rotational constants are functions of the squares of the distances, the signs of the coordinates are not determined. In oxaspiropentane the signs were taken from the model structure. A possible ambiguity existed, however, in the  $c$  coordinate of the  $\text{C}_5$  atom whose magnitude is small enough to warrant investigation of the alternate choice of sign. The structural calculation was therefore repeated with the sign of the coordinate taken as positive. The results clearly showed that the initial choice was correct, since the second calculation yielded unreasonable values for the bond distances and angles. For example,  $r(\text{C}_5\text{-O})$  was calculated to be 1.28 Å and the two  $\text{C}_3\text{-H}_b$ ,  $\text{H}_c$  distances differed by 0.07 Å. The deviation of the least-squares fit

Table III. Comparison of Rotational Constants and Coordinates Using Inertial Defect

	Obsd <sup>a</sup>	<sup>13</sup> C <sub>2</sub> calcd from eq 1	Diff	Obsd	<sup>13</sup> C <sub>5</sub> calcd from eq 1	Diff
A	11497.045	11496.446	0.599	11614.440	11614.638	-0.198
B	4314.287	4313.689	0.598	4394.981	4395.179	-0.198
C	4259.635	4259.037	0.598	4321.662	4321.860	-0.198
a <sup>b</sup>	-1.3032	-1.3091	0.0059	0.0174	0.0173	0.0001
b	0.0	0.0	0.0	0.0	0.0	0.0
c	-0.6859	-0.6867	0.0008	-0.0943	-0.0928	-0.0015
		$I_a + I_c - I_b$		$\Delta I_a + \Delta I_c - \Delta I_b^c$		
	<sup>12</sup> C	45.46266		0.0		
	<sup>13</sup> C <sub>2</sub>	45.45995		0.00271		
	<sup>13</sup> C <sub>5</sub>	45.46358		-0.00092		

<sup>a</sup> Rotational constants calculated from complete set of transitions (Q and R branches). Units are in MHz. <sup>b</sup> Coordinates (in Å) calculated from rotational constants by Kraitchman's equations or moment equations. <sup>c</sup>  $\Delta I_a = I_a(^{12}\text{C}) - I_a(\text{isotope})$ , etc.

Table IV. Atomic Coordinates for Oxaspiro[2.2]pentane<sup>a</sup>

Atom <sup>b</sup>	a	b	c
C <sub>5</sub>	-0.0174 ± 0.0088	0.0	-0.0943 ± 0.0001
C <sub>2</sub>	1.3032 ± 0.0001	0.0	-0.6859 ± 0.0001
H <sub>a</sub>	1.7140 ± 0.0001	-0.9259 ± 0.0001	-1.0778 ± 0.0001
H <sub>a</sub> '	1.7140 ± 0.0001	0.9259 ± 0.0001	-1.0778 ± 0.0001
O	1.1100 ± 0.0027	0.0	0.7616 ± 0.0030
C <sub>3</sub>	-1.2646 ± 0.0001	-0.7751 ± 0.0001	-0.0242 ± 0.0027
H <sub>b</sub>	-1.5051 ± 0.0001	-1.2607 ± 0.0001	0.9039 ± 0.0001
H <sub>c</sub>	-1.6132 ± 0.0001	-1.2857 ± 0.0001	-0.9104 ± 0.0001
C <sub>4</sub>	-1.2646 ± 0.0001	0.7751 ± 0.0001	-0.0242 ± 0.0027
H <sub>c</sub> '	-1.5051 ± 0.0001	1.2607 ± 0.0001	0.9034 ± 0.0001
H <sub>b</sub> '	-1.6132 ± 0.0001	1.2857 ± 0.0001	-0.9104 ± 0.0001

<sup>a</sup> All coordinates and errors in Å. Errors listed represent errors in rotational constant least-squares fit propagated through Kraitchman's equations. Errors for coordinates not directly determined (i.e., a(C<sub>2</sub>), a(O), c(O), and c(C<sub>3,4</sub>)) are from deviation of least-squares fit of moment equations. Errors less than 10<sup>-4</sup> set equal to 1 × 10<sup>-4</sup>. <sup>b</sup> See Figure 1 for atom labeling.

was also larger by an order of magnitude for the alternate sign choice. The structural parameters derived from the final set of coordinates are given in Table V as structure IA.

The exclusive use of Kraitchman's equations in structure determination is to be preferred in that only differences in moments are used, thus partially canceling vibrational effects. The coordinates that are obtained by solution of the moment equations are less accurate as they must absorb the errors that arise from using relations that are strictly valid only for rigid molecules. To assess the structural contributions of these effects, the experimental data were further analyzed in several ways.

A second calculation involved a least-squares fit of the data from all seven species to the second moment equations<sup>15</sup> and center-of-mass conditions. The results, labeled structure IIA in Table V, are equivalent to an *r*<sub>0</sub> structure and do not involve the use of Kraitchman's equations. A similar calculation, labeled IIIA, used the second moment differences between parent and isotopic species in the least-squares analysis. All three of these calculations were re-

Table V. Comparison of Structural Parameters as Calculated by Several Techniques

Parameter <sup>a</sup>	IA <sup>b</sup> (preferred)	Difference <sup>c</sup>						Standard deviation <sup>d</sup>
		IB	IIA	IIB	IIIA	IIIB	IV	
C <sub>2</sub> -H <sub>5</sub>	1.447	0.001	-0.011	-0.007	-0.004	0.000	0.000	0.006
C <sub>2</sub> -H	1.086	0.000	0.000	0.000	0.000	-0.001	-0.001	0.001
C <sub>2</sub> -O	1.460	0.001	0.004	0.004	0.002	0.003	0.004	0.004
C <sub>3</sub> -C <sub>4</sub>	1.550	0.000	0.002	0.002	0.003	0.003	-0.001	0.002
C <sub>3</sub> -H <sub>b</sub>	1.080	0.000	-0.002	-0.002	0.001	0.000	0.001	0.001
C <sub>3</sub> -H <sub>c</sub>	1.075	-0.000	0.002	0.002	-0.002	-0.001	-0.001	0.002
C <sub>5</sub> -C <sub>3</sub>	1.470	-0.001	0.015	0.012	0.002	0.000	-0.002	0.009
C <sub>5</sub> -O	1.416	0.002	-0.015	-0.013	0.006	0.005	0.005	0.010
∠HC <sub>2</sub> H	117.0	0.00	0.04	0.06	0.04	0.08	0.10	0.07
∠HC <sub>3</sub> H	115.0	0.00	0.14	0.16	0.11	0.12	0.11	0.13
∠C <sub>2</sub> OC <sub>5</sub>	60.4	-0.02	-0.27	-0.14	-0.38	-0.20	-0.17	0.25
∠C <sub>2</sub> C <sub>5</sub> O	61.3	-0.06	0.78	0.67	0.06	0.02	0.04	0.46
∠C <sub>3</sub> C <sub>5</sub> C <sub>4</sub>	63.6	0.06	-0.59	-0.45	0.01	0.14	0.04	0.34
∠C <sub>5</sub> C <sub>2</sub> O	58.3	0.07	-0.53	-0.54	0.31	0.15	0.15	0.38
∠C <sub>5</sub> C <sub>3</sub> C <sub>4</sub>	58.2	-0.03	0.27	0.23	-0.01	0.03	0.02	0.16
∠α <sup>e</sup>	9.61	0.03	-0.21	-0.15	-0.06	0.33	0.58	0.32
∠β <sup>f</sup>	9.75	0.00	0.25	-0.02	0.89	0.31	0.21	0.45
∠θ <sup>g</sup>	1.57	0.01	-0.14	-0.07	0.03	0.11	-0.02	0.09
∠φ <sup>h</sup>	0.68	-0.02	0.08	0.15	-0.32	-0.14	-0.16	0.17
∠τ <sup>i</sup>	0.24	0.02	-0.03	-0.13	0.45	0.20	0.17	0.24
			Additional Parameters					
∠HC <sub>2</sub> C <sub>5</sub> = 119.5 ± 0.1			∠H <sub>b</sub> C <sub>3</sub> C <sub>4</sub> = 116.9 ± 0.1			∠C <sub>2</sub> C <sub>5</sub> C <sub>3</sub> = 142.5 ± 0.2		
∠HC <sub>3</sub> O = 114.1 ± 0.1			∠H <sub>c</sub> C <sub>3</sub> C <sub>5</sub> = 118.0 ± 0.3			∠C <sub>4</sub> C <sub>5</sub> O = 130.3 ± 0.3		
∠H <sub>b</sub> C <sub>3</sub> H <sub>5</sub> = 118.9 ± 0.2			∠H <sub>c</sub> C <sub>3</sub> C <sub>4</sub> = 116.9 ± 0.1					

<sup>a</sup> See Figure 1 for atom labeling. <sup>b</sup> See text for definitions of structures IA, IB, etc. <sup>c</sup> Value of parameter from structure IB, etc., minus value of parameter from preferred structure IA. <sup>d</sup> Standard deviation of "differences" in columns IB-IV. <sup>e</sup> Angle between plane HC<sub>2</sub>H and bisector of ∠C<sub>2</sub>C<sub>5</sub>O. Methylene group moved toward oxygen. <sup>f</sup> Angle between plane C<sub>3</sub>C<sub>4</sub>C<sub>5</sub> and bisector of ∠C<sub>2</sub>C<sub>5</sub>O. <sup>g</sup> Angle formed by projection of ∠HC<sub>3</sub>H bisector onto the C<sub>3</sub>C<sub>4</sub>C<sub>5</sub> plane and bisector of ∠C<sub>5</sub>C<sub>3</sub>C<sub>4</sub>. Methylene groups moved toward each other. <sup>h</sup> Angle between bisector of ∠HC<sub>3</sub>H and its projection onto the C<sub>3</sub>C<sub>4</sub>C<sub>5</sub> plane. Methylene bisectors moved toward oxygen. <sup>i</sup> Twist angle about ∠HC<sub>3</sub>H bisector, defined as the angle between the normal to the HC<sub>3</sub>H plane and the projection of the normal onto the C<sub>3</sub>C<sub>4</sub>C<sub>5</sub> plane.

Table VI. Stark Measurements and Dipole Moment

Transition	<i>M</i> component	$(\Delta\nu\epsilon^2)^a \times 10^6$	
		Obsd	Calcd <sup>b</sup>
1 <sub>01</sub> → 2 <sub>11</sub>	0	2.872 ± 0.101	2.868
2 <sub>02</sub> → 3 <sub>03</sub>	0	-1.038 ± 0.018	-1.010
2 <sub>02</sub> → 3 <sub>03</sub>	1	4.235 ± 0.024	4.254
2 <sub>12</sub> → 3 <sub>13</sub>	0	3.064 ± 0.014	3.050
2 <sub>11</sub> → 3 <sub>12</sub>	0	1.451 ± 0.011	1.454
Principal axes		Molecular axes <sup>c</sup>	
$\mu_a = 0.840 \pm 0.012$		$\mu_x = 0.063 \pm 0.001$	
$\mu_b = 0.0$		$\mu_y = 0.0$	
$\mu_c = 1.721 \pm 0.004$		$\mu_z = 1.914 \pm 0.009$	
$\mu = 1.915 \pm 0.009$			

<sup>a</sup> Units are MHz V<sup>-2</sup> cm<sup>2</sup>. Conversion factor  $\mu\epsilon = 0.50344$  MHz D<sup>-1</sup> V<sup>-1</sup> cm. <sup>b</sup> From least-squares fit of observed data and stated dipole components. <sup>c</sup> See text for definition of axis system.

peated using the moments of inertia rather than the second moments, resulting in structures IB, IIB, and IIIB, respectively. These calculations are summarized in Table V. The entries in a given column represent the differences in structural parameters between structure IA and those calculated for the structure in that column.

An additional calculation which allows the estimation of the vibrational contributions to the moments of inertia involved determination of the effects of an arbitrary change in bond length upon isotopic substitution. A decrease of  $5 \times 10^{-5}$  Å for bonds between heavy atoms (C-C, C-O) and  $1 \times 10^{-4}$  Å for C-H bonds was assumed<sup>16a,b</sup> and calculation IA repeated using moments adjusted in this way. The differences in structural parameters between this calculation, IV, and IA, given in Table V, are thought to represent an upper limit of the vibrational contribution to the structure.

The various calculations described above show, as expected, that the *r*<sub>0</sub>-type structures (IIA,B) are farthest from the *r*<sub>s</sub>-type structure (IA). Those parameters derived from the moment differences (IIIA,B) are similar in theory to Kraitchman's technique and are generally in closer agreement with the *r*<sub>s</sub> results. The structures determined as described above, using the adjusted moments (IV), are also closer to IA. As expected, structures based on the use of either the moments of inertia or second moments are quite similar. Structure IA is preferred in that it is not only a substitution structure but also gave the best fit in the least-squares calculations.

The error limits for the final structure, given in the last column of Table V, are the standard deviations of the differences listed in columns IB-IV in the table and are felt to reflect the maximum uncertainties introduced by zero-point vibrational effects.

### Dipole Moment

Because of the numerous *K*<sub>a</sub> doublet near degeneracies connected by the *a* dipole in oxaspiropentane, many of the observed transitions exhibited mixed first- and second-order Stark effects. This was especially true for low *J* transitions. In order to accurately measure the dipole moment, only those *M* components having second-order Stark effects were used in the determination, as these are less sensitive to errors in the applied voltage. Most measurements were made on the *M* = 0 Stark component, for which the first-order effect vanishes. Because the second-order lines often move slowly with electric field, the base of the modulating square wave was floated while the peak was set at 1,000–4,000 V/cm above the base, allowing Stark components to be observed even at low voltage without interference from the zero-field line.

The  $|M| = 1$  component of the 2<sub>0,2</sub>-3<sub>0,3</sub> transition was also measured, in that it is the only low *J* line for which first-order Stark contributions are prohibited by symmetry. The electric field was calibrated at each voltage with carbonyl sulfide ( $\mu = 0.71521$ ),<sup>17</sup> which was admitted into the Stark cell with the sample. Taking the  $\mu_b$  component of oxaspiropentane as zero by symmetry, the  $\mu_a$  and  $\mu_c$  components are found by least-squares fit of the Stark coefficients. The results are given in Table VI.

The dipole moments of several related molecules are listed in Table VII. For purposes of comparison, the components have been transformed to a common molecular axis system in which the *x* axis lies along the epoxide ring C-C bond, the *y* axis is perpendicular to the plane of this ring, and the *z* axis is perpendicular to the epoxide ring C-C bond and through the oxygen atom. The dipole components listed in Table VII are given in this axis system.

The dipole moment of oxaspiropentane is consistent with those of ethylene oxide and the other related molecules in Table VII. The component along the *z* axis is nearly constant in this series of molecules and is responsible for almost all of the net dipole moment. Interestingly, the *z* components of the dipole moments of the methyl oxiranes increase regularly with increasing substitution, but oxaspiropentane's *z* component is 0.2 D smaller than the estimated number for the analogous 2,2-dimethyloxirane. The *x* component of the oxaspiropentane is also slightly smaller than expected from the methyl oxiranes. These effects are also reproduced in the CNDO/2 calculated dipole moments (Table VII).

### Discussion

The unique and highly strained geometry of the spiro[2.2]pentane ring system makes its detailed structure particularly interesting. The strain energy of spiro[2.2]pentane has been found to be very high at 65 kcal/mol. This strain energy is 9 kcal/mol higher than that of two independent cyclopropane rings.<sup>18a</sup> This extra ring strain makes the spiro[2.2]pentane and oxaspiro[2.2]pentane systems especially reactive.<sup>2</sup> For example, the activation energy for thermal rearrangement of spiro[2.2]pentane is 58 kcal/mol, 5–7 kcal/mol lower than for cyclopropane or 1,1-dimethylcyclopropane.<sup>18b</sup>

The strained geometry of oxaspiro[2.2]pentane would be expected to cause large deviations from the normal sp<sup>3</sup> hybridization at saturated carbons. By symmetry the central carbon, C<sub>5</sub>, should maintain approximate sp<sup>3</sup> hybridization, but the other carbons (C<sub>2</sub>, C<sub>3,4</sub>) should have a higher fraction of *p* character for the internal C-C bonds and a higher fraction of *s* character for the C-H bonds. From correlations of the NMR <sup>13</sup>C-<sup>13</sup>C spin-spin coupling constants in spiro[2.2]pentane with other molecules, the hybridization at the external carbons is thought to be about sp<sup>5.7</sup> (0.15 *s*) for the internal C-C bond.<sup>6</sup> From the 118.4° HCH bond angle in spiro[2.2]pentane,<sup>5</sup> the hybridization at carbon in the C-H bonds should be sp<sup>2.1</sup> (0.32 *s*) assuming that the C-H bonds are not bent.<sup>19</sup> This leaves the hybridization in the external C-C bond at sp<sup>3.8</sup> (0.21 *s*) (see Figure 2). Similar hybridizations would be expected for oxaspiro[2.2]pentane. In view of these expectations, a number of interesting correlations can be found between the structural parameters of oxaspiropentane and those of model compounds such as oxiranes and cyclopropanes, as given in Table VIII.

In oxaspiropentane, the internal C<sub>3</sub>C<sub>5</sub>C<sub>4</sub> and C<sub>2</sub>C<sub>5</sub>O angles are found to be larger than the corresponding angles in cyclopropane<sup>4</sup> and ethylene oxide<sup>3</sup> (Table VIII). The angle equivalent to C<sub>3</sub>C<sub>5</sub>C<sub>4</sub> increases from 60° in cyclopropane to 62.2° in spiro[2.2]pentane and to 63.6° in oxaspiropentane. This



Table VII. Comparison of Experimental Dipole Moments

Molecule		Dipole moment <sup>a</sup>			
		$\mu_x$	$\mu_y$	$\mu_z$	$\mu_{total}$
Oxirane <sup>b</sup>	Exptl	0.0	0.0	1.88 ± 0.01	1.88 ± 0.01
	CNDO <sup>c</sup>	0.0	0.0	2.04	2.04
2-Methyloxirane <sup>d</sup>	Exptl	0.22 ± 0.01	0.09 ± 0.01	1.98 ± 0.01	2.00 ± 0.02
	CNDO <sup>c</sup>	0.16	0.05	2.13	2.14
<i>cis</i> -2,3-Dimethyl-oxirane <sup>e</sup>	Exptl	0.00	0.32 ± 0.02	2.01 ± 0.02	2.03 ± 0.02
<i>trans</i> -2,3-Dimethyl-oxirane <sup>f</sup>	Exptl	0.00	0.00	2.03 ± 0.04	2.03 ± 0.04
2,2-Dimethyloxirane	(Estimated) <sup>g</sup>	0.4	0.0	2.1	2.1
	CNDO <sup>c</sup>	0.32	0.0	2.15	2.17
Oxaspiro[2.2]pentane	Exptl	0.063 ± 0.001	0.0	1.914 ± 0.009	1.915 ± 0.001
	CNDO <sup>c</sup>	0.15	0.0	2.04	2.04

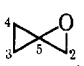
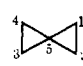


<sup>a</sup> Dipole components are given in the following molecular axis system: *x* axis through the ring C–C bond, *y* axis perpendicular to the ring plane, and *z* axis through the oxygen atom and perpendicular to the C–C bond. <sup>b</sup> G. L. Cunningham, Jr., A. W. Boyd, R. J. Myers, W. D. Gwinn, and W. I. LeVan, *J. Chem. Phys.*, 19, 676 (1951). <sup>c</sup> By the method of J. A. Pople and M. Gordon, *J. Am. Chem. Soc.*, 89, 4253 (1967). <sup>d</sup> J. D. Swalen and D. R. Herschbach, *J. Chem. Phys.*, 27, 100 (1957). <sup>e</sup> M. L. Sage, *ibid.*, 35, 142 (1961). <sup>f</sup> M. R. Emptage, *ibid.*, 47, 1293 (1967). <sup>g</sup> Estimated dipole components extrapolated from experimental value of oxirane and methyloxirane.

is also reflected by a 0.031 Å increase in the C<sub>3</sub>–C<sub>4</sub> bond length of oxaspiropentane over that of spiropentane and a 0.041 Å increase with respect to cyclopropane.<sup>20</sup> Similarly, the C<sub>2</sub>C<sub>5</sub>O angle increases from 59.2° in ethylene oxide to 61.3° in oxaspiropentane, with the increase in C<sub>2</sub>–O distance being 0.032 Å.<sup>20</sup> These effects can be attributed to the symmetrically strained spiro carbon atom (C<sub>5</sub>) which by symmetry must nearly maintain sp<sup>3</sup> hybridization. These sp<sup>3</sup> orbitals are bent far from the internuclear lines, and, in order to maintain optimal overlap with the sp<sup>3</sup> orbitals, the C<sub>3</sub>C<sub>5</sub>C<sub>4</sub> and C<sub>2</sub>C<sub>5</sub>O angles increase to greater than 60°. The C<sub>3</sub>C<sub>4</sub>C<sub>5</sub> angle decreases and the hybridizations for the internal bonds at O, C<sub>2</sub>, C<sub>3</sub>, and C<sub>4</sub> assume a great deal of p character. This is reflected in a decrease in the p character of the C–H bonds, for which the hybridizations have been calculated from the HCH bond angles<sup>19</sup> to be sp<sup>2.4</sup> (0.30 s) and sp<sup>2.1</sup> (0.31 s) for C<sub>3,4</sub>–H and C<sub>2</sub>–H, respectively. These are nearly equal to the hybridizations calculated for the C–H bonds in spiropentane (Figure 2).



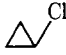
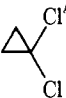
The orientation of the methylene groups on the cyclopropane ring of oxaspiropentane also appears to show the effect of the C<sub>5</sub> atomic hybridization. The bisector *d* of the –CH<sub>2</sub> group is displaced from the bisector of the cyclopropane ring angle by 1.57° (denoted by  $\theta$  in Figure 1) in such a way that the –CH<sub>2</sub> groups approach each other. This could be interpreted as resulting from the optimization of orbital overlap with the widely spread sp<sup>3</sup> orbitals of the C<sub>5</sub> atom. This would at the same time decrease the bending in the C<sub>3</sub>–C<sub>4</sub> bond and increase the C<sub>3</sub>–C<sub>4</sub> orbital overlap. Spiropentane also shows this effect, with the –CH<sub>2</sub> groups being displaced toward each other by 2.3°. From <sup>13</sup>C–<sup>13</sup>C spin-spin coupling constant results<sup>6</sup> as shown in Figure 2, it appears that the C<sub>3</sub>–C<sub>4</sub> bonding orbitals have higher s character than the C<sub>3</sub> and C<sub>4</sub> orbitals directed toward C<sub>5</sub>.

As can be seen from Table VIII, the methylene angles and C–H distances in oxaspiropentane are quite similar to those found in cyclopropane and ethylene oxide. The values for the epoxide methylene (C<sub>2</sub>–H) in oxaspiropentane are identical with those recently determined for ethylene oxide by Hirose.<sup>3</sup> The C<sub>3</sub> methylene angle is very close to that determined for cyclopropane, but it is curious that this is smaller by 3.4° than that found in spiropentane. The two nonequivalent C–H bond lengths of the C<sub>3</sub> methylene groups are unusual. They are slightly different from each other (by 0.005 Å, although some of this may be attributed to zero-point vibrational effects) and both are shorter than the bond lengths for the related molecules, spiropentane and cyclopropane. In oxaspiropentane, the cyclopropane

Table VIII. Comparison of Structural Parameters of Oxaspiropentane with Corresponding Parameters in Analogous Molecules

Parameter <sup>a</sup>				
$r(C_3-C_5)$	1.470	1.469	1.509	
$r(C_3-C_4)$	1.550	1.519	1.509	
$r(C_2-C_5)$	1.447			1.462
$r(C_5-O)$	1.415			1.428
$r(C_2-O)$	1.460			1.428
$\angle C_3C_2O$	58.3			59.2
$\angle C_2C_5O$	61.3			59.2
$\angle C_2OC_5$	60.4			61.6
$\angle C_3C_5C_4$	63.6	62.2	60.0	
$\angle C_4C_3C_5$	58.2	58.9	60.0	
$\angle HC_2H$	117.0			116.9
$\angle HC_3H$	115.0	118.4	115.1	
$r(C_3-H_c)$	1.075	1.091	1.088	
$r(C_3-H_b)$	1.080	1.091	1.088	
$r(C_2-H)$	1.086			1.086
$\angle \alpha^e$	9.61			7.97
$\angle \beta^e$	9.75			

HCH parameter <sup>e</sup>				
$\theta$ (in-plane)	1.57	2.3	–1.88	3.96
$\varphi$ (out-of-plane)	0.68		1.22	
$\tau$ (twist)	0.24		–0.36	

<sup>a</sup> The parameters analogous to oxaspiropentane are tabulated for cyclopropane and ethylene oxide. <sup>b</sup> Reference 5. <sup>c</sup> Reference 4. <sup>d</sup> Reference 3. <sup>e</sup> Parameter is defined in footnote of Table V and shown in Figure 1. <sup>f</sup> Reference 21. <sup>g</sup> Reference 26.

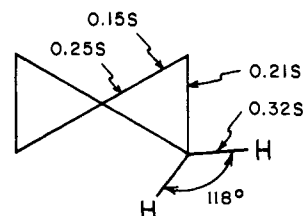


Figure 2. Fractions of s character in bonds of the spiro[2.2]pentane ring system.

–CH<sub>2</sub> groups exhibit a slight out-of-plane tilt ( $\varphi$  in Figure 1) which moves the groups toward the oxygen atom by



0.65°. This is also seen in chlorocyclopropane for which the  $-\text{CH}_2$  group is tilted toward the electronegative chlorine by 1.22°. The cyclopropane methylene groups in oxaspiropentane are twisted about their bisectors ( $\tau$  in Figure 1) by a very small amount (0.24°) which moves the  $\text{H}_c$  atoms toward each other, but again this may be an artifact attributable to vibrational effects.

Another interesting structural feature in oxaspiropentane involves the orientation of the  $\text{C}_2$  methylene and cyclopropyl groups attached to the epoxide ring. The bisectors of these groups deviate from the bisectors of the epoxide ring angles ( $\alpha$  and  $\beta$  in Fig. 1) by 9.61 and 9.75°, respectively. This effect is also found in ethylene oxide, in which the methylene groups are rotated toward the oxygen atom by 7.91°, and to a lesser degree in cyclopropanes with electronegative substituents.<sup>3,22</sup> It appears to be most pronounced, however, in the highly strained oxaspiropentane.

It has been previously noted that the oxaspiropentane  $\text{C}_3\text{C}_5\text{C}_4$  bond angle is increased with respect to that in cyclopropane. This is also seen in spiropentane for which the corresponding angle is increased from the cyclopropane value of 60 to 62.2°. In oxaspiropentane, however, an even greater increase, to 63.6°, is seen with a corresponding increase in the  $\text{C}_3\text{--C}_4$  distance to 1.550 Å. This is an unusually long  $\text{C--C}$  distance for an unconstrained three-membered ring.<sup>3,23</sup> The  $\text{C}_5$  hybridization effect does not appear to account for the total increase in this value. The relative lengths of the  $\text{C--C}$  bonds in other cyclopropyl derivatives have been shown to vary with the electronic nature of the substituent.<sup>24</sup> For  $\pi$  electron withdrawing substituents, this effect has been explained by Hoffmann in terms of a net transfer of electrons out of the cyclopropyl ring to the low-lying  $\pi$  orbitals of the substituent. However, a  $\pi$ -donating substituent, such as oxygen or fluorine presumably acts to furnish  $\pi$  electrons to the cyclopropane antibonding orbital, resulting in a net decrease in the  $\text{C}_3\text{--C}_4$  bond strength.<sup>24</sup> This, then, could account for the additional increase in the  $\text{C}_3\text{--C}_4$  bond length observed in oxaspiropentane. Similar effects have recently been noted in difluorocyclopropane.<sup>25</sup>

Another substituent effect can be observed in the chloro-substituted cyclopropanes in which the methylene groups are pushed away from each other with the size of this angle ( $\theta$  in Table VIII) nearly doubling on going from chlorocyclopropane to dichlorocyclopropane.<sup>26</sup> This contrasts with oxaspiropentane and spiropentane, in which the methylene groups approach each other. The oxygen atom may have an effect similar to that of the chlorine substituents which could explain the smaller  $\theta$  value observed in oxaspiropentane relative to that in spiropentane.

**Acknowledgment.** We are grateful to Dr. R. H. Schwendeman for his comments and for the use of his general structure fit computer program. We would also like to thank Dr. M. D. Harmony for his suggestions regarding zero-point vibrational effects. The original centrifugal distortion program was kindly supplied by Dr. T. Tanaka. This work was supported in part by National Science Foundation Grant No. MPS 72-04978-AOJ and acknowledgment is made to the donors of The Petroleum Research Fund, administered by the American Chemical Society, for partial support.

**Supplementary Material Available.** A listing of microwave frequencies including centrifugal distortion corrections for the assigned transitions of the six isotopic species will appear following these pages in the microfilm edition of this volume of the Journal. Photocopies of the supplementary material from this paper only or microfiche (105 X 148 mm, 24X reduction, negatives) containing all the supplementary material for the papers of this issue may be obtained from the Business Office, Books and Journals Division, American Chemical Society, 1155 16th St., N.W., Washington, D.C. 20036. Remit check or money order for \$4.50 for photocopy or \$2.50 for microfiche, referring to code number JACS-75-6638.

## References and Notes

- (1) (a) Quantum Institute; (b) Department of Chemistry.
- (2) (a) D. H. Aue, M. J. Meshishnek, and D. F. Shellhamer, *Tetrahedron Lett.*, 4799 (1973), and references therein; (b) J. R. Salau and J. M. Conla, *Chem. Commun.*, 1579 (1971); (c) B. M. Trost and M. J. Bogdanowicz, *J. Am. Chem. Soc.*, **95**, 5321 (1973), and references therein.
- (3) C. Hirose, *Bull. Chem. Soc. Jpn.*, **47**, 1311 (1974).
- (4) O. Bastiansen, F. N. Fritsch, and K. Hedberg, *Acta Crystallogr.*, **17**, 538 (1964).
- (5) G. Dallinga, R. K. Van Der Draai, and L. H. Toneman, *Recl. Trav. Chim. Pays-Bas*, **87**, 897 (1968).
- (6) (a) R. D. Bertrand, D. M. Grant, E. R. Alfred, J. C. Hinshaw, and A. B. Strong, *J. Am. Chem. Soc.*, **94**, 997 (1972); (b) H. Gunther, *Chem. Ber.*, **106**, 3938 (1973).
- (7) L. H. Scharpen and V. W. Laurie, *J. Chem. Phys.*, **49**, 221 (1968).
- (8) (a) P. S. Dowd, *Acc. Chem. Rec.*, **5**, 242 (1972); (b) M. J. S. Dewar and J. S. Wasson, *J. Am. Chem. Soc.*, **93**, 3091 (1971); (c) W. T. Borden and L. Salem, *ibid.*, **95**, 932 (1973); (d) W. J. Hehre, L. Salem, and M. R. Willcott, *ibid.*, **96**, 4328 (1974).
- (9) D. H. Aue and M. J. Meshishnek, to be published.
- (10) R. F. Curl, Jr., *J. Comput. Phys.*, **6**, 367 (1970).
- (11) J. Kraitzman, *Am. J. Phys.*, **21**, 17 (1953).
- (12)  $(A - C)/2$  and  $\kappa = (2B - A - C)/(A - C)$ .
- (13) D. Kivelson and E. B. Wilson, Jr., *J. Chem. Phys.*, **20**, 1575 (1952).
- (14) W. H. Kirchhoff, *J. Mol. Spectrosc.*, **41**, 333 (1972).
- (15) The second (planar) moments are defined as  $P_a = \sum_i m_i a_i^2$ ,  $P_{ab} = \sum_i m_i a_i b_i$ , etc., and are related to the moments of inertia as follows:  $P_a = \frac{1}{2}(I_b + I_c - I_a)$ , etc. (ref 11).
- (16) (a) V. W. Laurie and D. R. Herschbach, *J. Chem. Phys.*, **37**, 1687 (1962); (b) R. D. Suenram and M. D. Harmony, *J. Am. Chem. Soc.*, **95**, 4506 (1973).
- (17) J. S. Meunier, *J. Chem. Phys.*, **48**, 4544 (1968).
- (18) (a) P. v. R. Schleyer, J. E. Williams, and K. R. Blanchard, *J. Am. Chem. Soc.*, **92**, 2377 (1970); (b) S. W. Benson and H. E. O'Neal, "Kinetic Data on Gas Phase Unimolecular Reactions", National Bureau of Standards, Washington, D.C., 1970, p 320.
- (19) These hybridizations are calculated assuming contributions from only one s and three p orbitals and using the relation  $\cos \theta = -1/(\delta\gamma)^{1/2}$ , where  $\theta$  is the angle between two orbitals of  $\text{sp}^\delta$  and  $\text{sp}^\gamma$  hybridization. The hybridizations calculated for cyclopropanes ( $\angle\text{HCH} \approx 116^\circ$ ) (Table VIII) are  $\text{sp}^{2.3}$  (0.30 s) for the  $\text{C--H}$  bonds and  $\text{sp}^{4.0}$  (0.20 s) for the  $\text{C--C}$  bonds. C. A. Coulson, "Valence", Oxford University Press, London, 1952, p. 194.
- (20) It has been previously pointed out that although the individual bond distances in cyclopropane rings may vary, the average  $\text{C--C}$  distance remains fairly constant, centered about the value of 1.509 Å found for cyclopropane; see ref 16b and R. D. Suenram and M. D. Harmony, *J. Chem. Phys.*, **56**, 3837 (1972). In the case of oxaspiropentane it appears that the average value for the cyclopropyl ring, 1.497 Å, is slightly smaller, being nearly equal to that found for the highly strained bicyclobutane (1.498 Å); the average value for spiropentane, 1.486 Å, is the smallest yet reported for a cyclopropane ring.
- (21) R. H. Schwendeman, G. D. Jacobs, and T. M. Krigas, *J. Chem. Phys.*, **40**, 1022 (1964).
- (22) A related effect is noted in  $\text{CH}_2\text{X}$  and  $\text{CH}_2\text{X}_2$  ( $\text{X} = \text{H}, \text{NF}_2, \text{F}, \text{Cl}, \text{Br}$ ), where the electronegative substituents show a slight increase in the  $\text{HCH}$  angle. The magnitude of this effect on these unstrained acyclic compounds, however, is not large enough to account for the large angle of tilt observed in the strained ring compounds; *Chem. Soc. Spec. Publ.*, **No. 11** (1958); **No. 18** (1965).
- (23) See K. B. Wiberg, G. J. Burgmaier, K. Shen, S. L. LaPlaca, W. C. Hamilton, and M. D. Newton, *J. Am. Chem. Soc.*, **94**, 7402 (1972), for a long  $\text{C--C}$  bond in a constrained cyclopropane ring.
- (24) R. Hoffmann, *Tetrahedron Lett.*, 2907 (1970); R. Hoffmann and R. B. Davidson, *J. Am. Chem. Soc.*, **93**, 5699 (1971).
- (25) A. T. Perretta and V. W. Laurie, presented at the Symposium on Molecular Structure and Spectroscopy, The Ohio State University, June 1973.
- (26) W. H. Flygare, A. Narath, and W. D. Gwinn, *J. Chem. Phys.*, **36**, 200 (1962).